Journal of Electron Spectroscopy and Related Phenomena 247 (2021) 147033

Contents lists available at ScienceDirect

Journal of Electron Spectroscopy and Related Phenomena

journal homepage: www.elsevier.com/locate/elspec

THE PHOTOELECTRON SPECTROSCOPY OF THE DICHLOROETHYLENES: THE VICINAL ISOMER trans-1,2-HClC=CHCl. QUANTUM CHEMICAL CALCULATIONS AND EXPERIMENT

R. Locht [a,*], D. Dehareng [b], B. Leyh [a]

[a] MolSys Research Unit, Laboratory for Molecular Dynamics, Department of Chemistry, Institute of Chemistry, Blg.B6c, University of Liège, Sart-Tilman, B-4000, Liège 1, Belgium

[b] Centre d'Ingéniérie des Protéines, Institute of Chemistry, Blg.B6a, University of Liège, Sart-Tilman, B-4000, Liège 1, Belgium

A B S T R A C T

The photoelectron spectrum (PES) of trans-1,2-$C_2H_2Cl_2$ has been measured with the resonance lines in He, Ne and Ar. These spectra are compared to the threshold photoelectron spectrum (TPES) recorded using synchrotron radiation. Nine mostly well separated photoelectron bands are observed at adiabatic ionization energies of 9.633 eV, 11.840 eV, 12.044 eV, 12.582 eV, 13.581 eV, 14.081 eV, 15.724 eV and at about 16.325 eV and 19.00 eV. Most of them exhibit a well resolved and extended vibrational structure. The He-I photoelectron band associated with the ground electronic state of the ion and the corresponding TPES band are characterized by a vibrational structure extending over 0.7 eV and 2.0 eV respectively. In the latter case the strong correlation between the TPES and the photoabsorption spectrum in the same energy region has been established. Several excited states also show an extended vibrational structure. The assignments of the electronic bands and of the vibrational wavenumbers were supported by quantum chemical calculations. The good correlation between predicted vibrational wavenumbers and the experimental values allowed us to assign most of the vibrational structures. The constant ion state (CIS) spectra have been recorded and discussed for selected vibrational levels of the ground state and for the adiabatic transition to the first excited state of the ion.

1. Introduction

We already investigated the photoelectron spectroscopy (PES) of the geminal 1,1- [1] isomer of dichloroethylene ($C_2H_2Cl_2$). Beside the HeI-(at 21.22 eV) PES, the photoelectron spectra excited by NeI- (at 16.67-16.85 eV) and ArI/ArII- (at 11.62-11.83 eV/13.48 eV) resonance lines were investigated. The threshold photoelectron spectrum (TPES) and constant ion state spectra (CIS) of this molecule using synchrotron radiation were also described and interpreted. In the literature most of the time the trans-1,2-$C_2H_2Cl_2$ investigation was associated to that of its two isomers [2–7].

The aim of the present paper is to report on a better resolved photoelectron spectrum of trans-1,2-$C_2H_2Cl_2$ with the HeI- but also with the NeI- and ArI/ArII- excitation lines. Using synchrotron radiation a better resolved TPES and new CIS spectra have been recorded. *Ab initio* quantum chemical calculations have been performed to assign the electronic bands and the individual vibrational wavenumbers of the cation in its ground and excited electronic states.

2. Experimental

2.1. Experimental setups

Two experimental setups were used in this work [8,9] and only the most important aspects will be documented here.

The fixed-wavelength (PES) experimental set-up used in this work is part of a PEPICO experiment [8]. The gaseous sample is introduced by an effusive gas inlet. Photoions and photoelectrons are extracted by a weak field (50 mV/cm). These particles are analyzed respectively in a quadrupole mass spectrometer and in a photoelectron energy analyzer described by Lindau et al. [10]. The photoelectron energy resolution, obtained under coincidence conditions, is 30 meV as measured on Ar^+/e- coincidence data.

Perpendicularly to the photoion-photoelectron optical axis, the light is provided by a discharge in He (HeI line: 58.43 nm or 21.22 eV), Ne (NeI lines: 73.58-74.37 nm or 16.850-16.671 eV) or Ar (ArI lines: 104.82-106.67 nm or 11.828-11.623 eV; ArII line: 91.97 nm or 13.480 eV) and is introduced in the ion chamber through a capillary of 0.5 mm diameter. A photoelectric light detector is placed opposite and coaxially to monitor the light source continuously.

* Corresponding author.
E-mail address: robert.locht@uliege.be (R. Locht).

https://doi.org/10.1016/j.elspec.2020.147033
Received 25 September 2020; Received in revised form 12 December 2020; Accepted 14 December 2020

For TPES and CIS experiments, the synchrotron radiation available from the BESSY II facility (Berlin, Germany), was dispersed at the 3m-NIM-2 beam line using a Pt-grating of 2400 lines/mm with an optimal transmission between 10 eV and 40 eV (124-31 nm). The entrance and exit slits were adjusted at 100 μm. A LiF filter (cutoff at 11.8 eV) removes second order contributions. The light beam is focused in the focusing plane of a tandem electron spectrometer consisting of two 180° electrostatic deflectors [9] working at constant energy resolution.

The TPES operating mode corresponds to "constant photoelectron energy" spectroscopy. The photon energy is scanned while the kinetic energy of the electrons travelling through the energy analyzer is kept as close as possible to zero, so that only "zero-kinetic energy" or "threshold" (TPE) photoelectrons are transmitted. The experimental conditions are tuned to maximize the TPE signal. A global photoelectron energy resolution of 4 meV is achieved at a pass-energy of 0.9 eV.

CIS spectroscopy allows measuring the relative partial ionization cross section of well-defined vibronic states of the molecular ion as a function of the incident photon energy. To record a CIS spectrum, a linked scan of the photon energy and the electron kinetic energy is performed to keep their difference constant and equal to the ionization energy for the selected vibronic state of the ion.

In addition to the synchrotron storage ring beam current, the photoelectron signal of a gold diode, inserted in the ion chamber, is measured in order to normalize the photoelectron signals to the monochromator transmission function. The CIS spectra have also to be normalized to the analyzer transmission function. This is achieved by recording the $Xe^+(^2P_{1/2})$ CIS spectrum.

The commercially available trans-1,2-$C_2H_2Cl_2$, purchased from Sigma-Aldrich and of 98% purity, has been used without further purification.

2.2. Data treatment and uncertainties evaluation

To characterize more accurately low intensity features superimposed on a strong continuum a subtraction procedure is applied. For this purpose, the experimental curve is severely smoothed to simulate the underlying continuum. The result is then subtracted from the original spectrum. The smoothing procedure consists in filtering the experimental curve by fast Fourier transform (FFT). The weak features emerge from a remaining strongly attenuated background. The resulting diagram will be called Δ-plot in the next sections. This data processing has been used extensively [1,11] and was thoroughly validated by Carbonneau and Marmet [12].

The experimental resolution of the fixed-wavelength PES has been improved to about 15 meV by iterative deconvolution [13–19]. The deconvolved spectra have been carefully compared to both the raw data and the TPES data (see below) to guarantee the absence of any spurious signal appearing through the numerical deconvolution procedure.

The calibration of the fixed-wavelength PES energy scale to an accuracy of 2 meV is performed with reference to known noble gas ionization energies using a mixed sample of noble gases (Ar, Kr and Xe) and trans-1,2-$C_2H_2Cl_2$.

The wavelength calibration of the 3m-NIM monochromator has been performed by using the Ar absorption spectrum between the $^2P_{3/2}$ and the $^2P_{1/2}$ ionic states. The accuracy of this calibration is better than 2 meV.

In the measurements between 9 eV and 24 eV photon energy, the TPES spectrum has been recorded with energy steps of 10 meV. The error on the energy position of a feature is estimated to be 6 meV. In the TPES spectra recorded between 9.5 eV and 20.5 eV an energy increment of 5 meV has been adopted. The error on the energy position of a feature is estimated to be of the order of 3 meV.

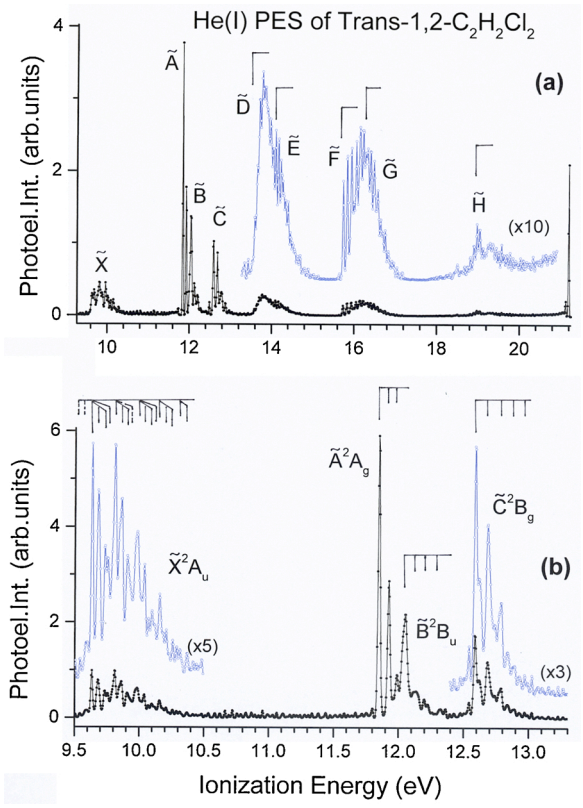

Fig. 1. HeI- PES of trans-1,2-$C_2H_2Cl_2$ between (a) 9.5 eV and 21 eV: vertical bars indicate the adiabatic ionization energies for the $\tilde{D} - \tilde{H}$ ionic states and (b) 9.5 eV and 13.5 eV: vertical bars indicate adiabatic ionization energies and the main vibrational structures.

3. Experimental Results

3.1. HeI-, NeI- and ArII/ArI-PES

The deconvoluted HeI-PES of trans-1,2-$C_2H_2Cl_2$ measured between 9.5 eV and 21 eV is displayed in Fig. 1a. Data on an expanded energy scale are shown in Fig. 1b in the 9.5-13.4 eV range with 4 meV increments. Electronic states and vibrational assignments are included.

Eight bands and one very weak high-energy band are observed between 9.5 and 21 eV and their adiabatic and vertical ionization energies are listed in Table 1 together with previously reported results obtained with HeI [2–4], HeII [6] and Al-Kα [5] excitation lines.

The NeI-PES of trans-1,2-$C_2H_2Cl_2$ is shown in Fig. 2a between 9.5 eV and 16.8 eV. Fig. 2b displays the 9.5-13.5 eV range on an expanded energy scale. In the same figure the HeI-PES is shown for comparison. It is normalized to the intensity at $IE_{ad} = 9.633$ eV. Several structures are marked by dotted lines to locate the probable contribution of the NeI-16.67 eV resonance line. The intensity ratio between NeI-(16.85/16.67 eV) is about 3:1 [20]. The fairly large differences compared to the HeI-PES will be addressed in section 5.

The ArI/ArII-PES of trans-1,2-$C_2H_2Cl_2$ is presented in Fig. 3. The probable contributions of the ArI-11.83/11.62 eV lines are indicated. In the same figure the HeI-PES is reproduced and normalized to the intensity at $IE_{ad} = 9.633$ eV. Strong differences are observed over the whole ionization energy range. These will also be discussed in section 5.

3.2. Threshold-PES

The TPES spectrum of trans-1,2-$C_2H_2Cl_2$ recorded with 5 meV energy increments is shown in Fig. 4a between 9.5 eV and 20.5 eV. For comparison the HeI-PES is reproduced in the same figure and normalized to

Table 1
Adiabatic (IE_{ad}) and vertical (IE_{vert}) ionization energies (eV) of trans-1,2-$C_2H_2Cl_2$ measured in this work by HeI-, NeI-, ArII-PES and by TPES using synchrotron radiation. A comparison is made with previously reported data using HeI- [2–4], Al-Kα [5], HeII- [6] and TPES [7].

[3]		[2]		[4]	[5]	[6]	[7]	This Work			
HeI		HeI		HeI	Al-Kα	HeII	TPES	HeI, NeI, ArII[a]		TPES[c]	
IE_{ad}	IE_{vert}	IE_{ad}	IE_{vert}	IE_{vert}	IE_{vert}	IE_{vert}	IE_{vert}	IE_{ad}	IE_{vert}	IE_{ad}	IE_{vert}
9.69	9.93	9.64	9.81	9.72	9.8	9.8	10.21	9.633(4)[b]	9.856	9.633[b]	10.176
11.68	11.94	11.86	11.86	11.79	11.9	11.9	11.88	11.840(8)	11.840	11.837	11.837
12.03	12.03	11.93	11.93	12.01	12.1	12.1	12.08	12.044(5)	12.044	12.043	12.043
12.57	12.66	12.61	12.61	12.55	12.7	12.7	12.77	12.582(6)	12.582	12.571	12.665
13.59	13.88		13.85	13.79	13.9	13.9	13.91	13.581(4)	13.774	13.579	13.764
	14.20		14.20	14.20	14.2	14.2	14.01	14.081(6)	14.169	14.087	14.167
15.62	16.15		16.23	16.19	16.2	16.3	16.28	15.725(6)	16.139	15.707	15.804
	17.41							16.325(5)	16.482	16.332	16.197
	19.10		~19.00	~19.0	19.0	19.2	18.99	19.00 (1)	19.00	18.977	18.977
					22.4	22.5					
					25.6	25.6					
					27.1	27.1					

[a] Excepting the first IE_{ad}, all the values are average values of the HeI-(up to 21.2 eV), NeI-(up to 16.8 eV) and ArII-(up to13.eV) spectra. The largest deviation from the average is mentioned in brackets.
[b] The first IE_{ad} value is given by the average over 15 measurements of HeI- (6), NeI-(2), ArII-(2)and TPES (5). The largest deviation from the average is given in brackets.
[c] The uncertainty estimated on the TPES data is ±0.005 eV.

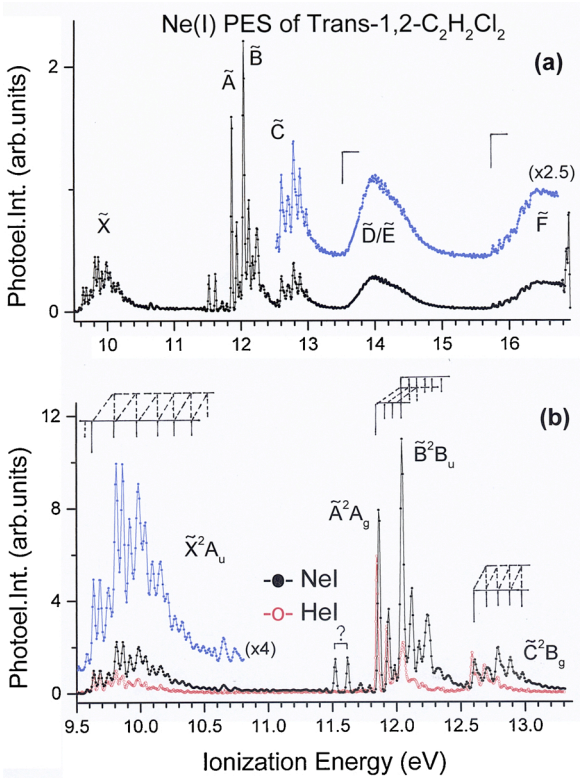

Fig. 2. NeI- PES of trans-1,2-$C_2H_2Cl_2$ between (a) 9.5 eV and 16.5 eV. (b) 9.5 eV and 13.5 eV. The HeI-PES normalized at 9.633 eV (red curve) is shown for comparison. Vertical bars show the major vibrational structure. Dashed lines correspond to NeI-16.67 eV contributions.

the intensity of the adiabatic transition in the first PES band. The vertical ionization energies determined in this spectrum are listed in Table 1 and compared with the results of Parkes et al. [7] using the same technique. The TPES obtained under the same conditions is shown on an expanded energy scale in Fig. 4b where the positions of the main structures are included.

As often observed, large differences between the HeI-PES and the TPES appear. Compared to the intensity of the $\tilde{X}^2A_u$ band of the ionic

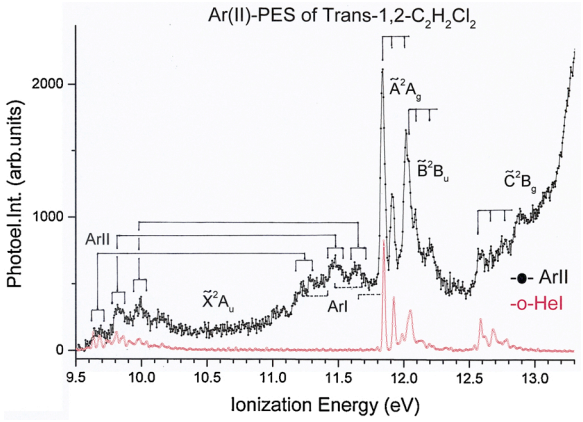

Fig. 3. ArII/ArI- PES of trans-1,2-$C_2H_2Cl_2$ between 9.5 eV and 13.5 eV. The ArI-line at 11.83-11.62 eV contributions are indicated. Vertical bars show the major vibrational structure. The HeI-PES normalized at 9.633 eV (red curve) is shown for comparison.

ground state at 9.633 eV, the relative intensities of the PES bands of the ionic excited states are considerably enhanced by resonant photoionization. Despite the higher resolution achieved in the TPES the vibrational structure appears strongly smoothed. This observation will be discussed in section 5.2.

3.3. The CIS spectra

The CIS spectra have been measured from threshold to 17 eV for the first two TPES bands. The result is illustrated in Fig. 5a together with the Δ-plot of the photoabsorption spectrum measured in the 12-17 eV energy range [21]. The chosen ionization energies correspond to the IE_{ad} (9.630 eV and 11.840 eV) of the first two electronic states and the TPES band maximum of the $\tilde{X}^2A_u$ state at 10.330 eV. The CIS at 11.140 eV corresponds to an energy lying outside the Franck-Condon region. Fig. 5b represents vibrationally resolved CIS spectra for the indicated internal energy of the molecular ion in its ground electronic state. The Δ-plot of the PAS between 9.5 eV and 12.2 eV has been included [21].

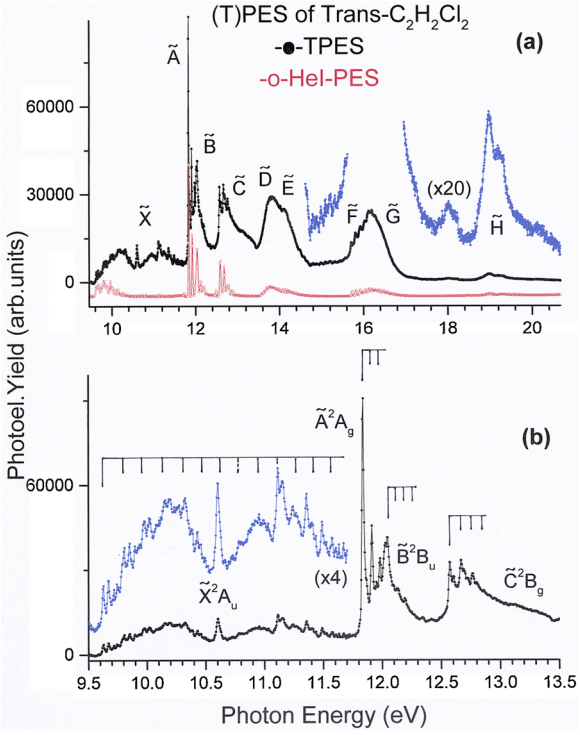

Fig. 4. TPES of trans-1,2-$C_2H_2Cl_2$ (a) between 9.5 eV and 21 eV photon energy. The HeI-PES (red curve) of trans-1,2-$C_2H_2Cl_2$ (normalized at 9.633 eV) is reproduced for comparison; (b) between 9.5 eV and 13.5 eV. Vertical bars indicate the adiabatic ionization energies and the major vibrational progressions.

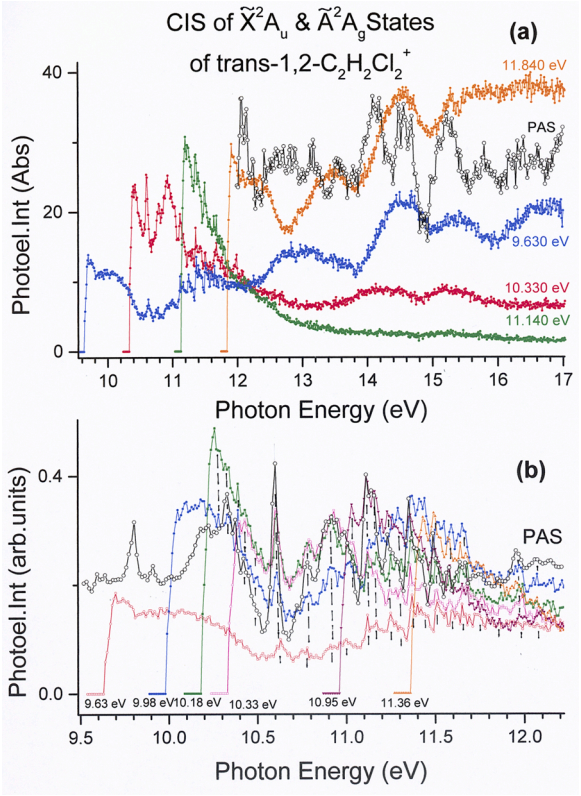

Fig. 5. CIS spectra of trans-1,2-$C_2H_2Cl_2^+$ (a) in the $\tilde{X}\ ^2A_u$ and $\tilde{A}\ ^2A_g$ states recorded at the indicated IE and the Δ-plot of the vacuum UV PAS between 12-17 eV [21]. (b) Vibrationally resolved CIS spectra of the $\tilde{X}\ ^2A_u$ [$v(\nu_2) = 0$-10] state at indicated IE's and Δ-plot of the vacuum UV PAS between 9.5 eV and 11.2 eV [21].

4. AB INITIO CALCULATIONS

4.1. Computational Tools

All calculations were performed with the Gaussian 09 program [22]. The basis set used for all the calculations is aug-cc-pVDZ [23] containing polarization and diffuse functions.

The geometry optimizations have been performed at the CCSD(FC) [24,25], M06-2X [26] and TDDFT(M06-2X) [27] levels.

The wavenumbers characterizing the twelve vibrational normal coordinates represented in Fig. S1 (see Supplementary material) have been determined at the M06-2X and TDDFT/ M06-2X levels.

The molecular orbital configuration of trans-1,2-$C_2H_2Cl_2$ in the neutral ground electronic state in the C_{2h} symmetry point group is described by:

$1s(Cl1)^2$, $1\,s(Cl2)^2$, $1\,s(C1)^2$, $1\,s(C2)^2$, $2\,s(Cl1)^2$, $2\,s(Cl2)^2$, $2p_{x,y,z}(Cl1)^6$, $2p_{x,y,z}(Cl2)^6$

$(1a_g)^2\ (1b_u)^2\ (2a_g)^2\ (2b_u)^2\ (3b_u)^2\ (3a_g)^2\ (4a_g)^2\ (1a_u)^2\ (1b_g)^2\ (4b_u)^2\ (5a_g)^2\ (2a_u)^2 : \tilde{X}\ ^1A_g$

This ordering of MO's agrees with that considered by Von Niessen et al. [6] using the outer valence Green's function method (OVGF). Using the same method built in Gaussian 03, Parkes et al. [7] obtained the reversed order for the $3a_g$ and $3b_u$ MO's. In their ESCA study Brendtsson et al. [5] used extended Hückel (EHT) and CNDO calculations which led to an inversion of the $1a_u$ and $4a_g$ MO's. To support their (e, 2e) spectroscopic analysis, Mei et al. [28] calculated the valence shell electronic configuration by restricted Hartree-Fock (RHF) at 6-31++/G** level resulting in the inversion of both the $1a_u$-$4a_g$ and $3a_g$-$3b_u$ MO's. In agreement with the present calculations, these authors mentioned that the $1a_u$ and $4a_g$ are nearly degenerate at this computational level. It should be noticed that in the present work only the excited states resulting from the ionization of one molecular orbital (MO) will be considered.

Recently, the analysis of Rydberg transitions observed in the vacuum UV-PAS of trans-1,2-$C_2H_2Cl_2$ [21] concluded on the basis of selection rules considerations that the probable MO sequence at increasing energy would be $4a_g$-$1a_u$ and $3a_g$-$3b_u$. This order will be adopted in the following sections.

4.2. Calculation Results

The result of the geometry optimization of the neutral $\tilde{X}\ ^1A_g$ ground state, the cationic ground $\tilde{X}\ ^2A_u$ and seven ionic excited states are presented in Table S1 (see Supplementary material), according to the atomic numbering shown in the figure below the table, at CCSD and M06-2X or TDDFT calculation levels. The $\tilde{C}\ ^2B_g$ and the $\tilde{D}\ ^2A_g$ ionic states have also been calculated in the C_S ($\tilde{C}\ ^2A''$) and C_2 ($\tilde{D}\ ^2A$) symmetry point groups respectively. When available, the results of previous *ab initio* calculations are also listed in the same table.

The wavenumbers of the vibrational normal modes involved in the eight cationic states are listed in Table 2. In this table a comparison with previous experimental and predicted data is presented for the ground electronic state of the neutral [29] and of the cation [30,31].

To the best of our knowledge only Takeshita [32] reported on the *ab initio* calculation of the wavenumbers associated with the vibrations belonging to the a_g representation in the $\tilde{A}\ ^2A_g$, $\tilde{B}\ ^2B_u$ and $\tilde{C}\ ^2B_g$ excited states of trans-1,2-$C_2H_2Cl_2^+$. This author calculated the ionization intensity curves including the vibrational structures of the four lowest ionic states and compared them with the experimental photoelectron spectrum.

The optimized geometries of the $\tilde{X}\ ^2A_u$, $\tilde{A}\ ^2A_g$, $\tilde{B}\ ^2B_u$, $\tilde{E}\ ^2A_u$, $\tilde{F}\ ^2A_g$ and $\tilde{G}\ ^2B_u$ states belong to the C_{2h} symmetry point group meaning that likely

Table 2
Experimental and calculated wavenumbers (cm^{-1}) of the vibrational normal modes (V.n.M) of trans-1,2-$C_2H_2Cl_2$ in its ground electronic state and of trans-1,2-$C_2H_2Cl_2^+$ in its ground and excited electronic states at different calculation levels and for different symmetry point groups.

V.n.M.	$\tilde{X}^1A_g$		$\tilde{X}^2A_u$			$\tilde{A}^2A_g$	$\tilde{B}^2B_u$	$\tilde{C}^2B_g$
M06-2X in C_{2h} point group								
	Exp. [29]	Calc.	[30] Exp.	Calc.	[31] Exp.	Calc.[a]	Calc.[a]	Calc.[a]	Calc.[a]
a_g								
ν_1	3073	3278	-	3121	-	3231	3112	3169	3267
ν_2	1578	1690	1452	1455	1451	1513	1543	1757	1719
ν_3	1274	1295	1258	1258	1257	1281	1224	1248	1273
ν_4	846	857	944	989	943	971	676	821	810
ν_5	350	358	367	365	368	372	305	347	336
a_u								
ν_6	900	953	871	855	836	849	879	905	927
ν_7	227	202	163	165	163	159	188	201	211
b_g								
ν_8	763	828	915	884	873	887	727	772	750
b_u								
ν_9	3090	3272	3121	3068	-	3228	3115	3099	3251
ν_{10}	1200	1217	1235	1244	1236	1250	1102	1037	1180
ν_{11}	828	841	-	1002	955	988	807	564	236
ν_{12}	250	243	-	244	251	243	248	100	**i96 C-Cl antis**

V.n.M.	$\tilde{A}^2A_g$	$\tilde{B}^2B_u$	$\tilde{C}^2B_g$		$\tilde{D}^2A_g$		$\tilde{E}^2A_u$	$\tilde{F}^2A_g$	$\tilde{G}^2B_u$
	TDDFT/M06-2X								
$C_S/C_2/C_{2h}$	C_{2h}	C_{2h}	C_{2h}	C_S	C_{2h}	C_2	C_{2h}	C_{2h}	C_{2h}
a'/a/a_g			TS		TS				
ν_1	3139	3177	3274	3286	3240	3105	3195	3479	3132
ν_2	1537	1725	1655	1689	1683	1413	1956	1888	1545
ν_3	1240	1252	1265	1270	1263	1009	1202	1419	1212
ν_4	721	816	785	843	787	729	640	813	716
ν_5	314	358	334	286	321	317	296	347	288
a"/b/a_u									
ν_6	913	929	913	925	257	886	1170	923	892
ν_7	**220**	220	187	189	**i743**	219	223	188	143
a"/b/b_g									
ν_8	742	780	747	632	752	711	776	616	691
a'/a/b_u									
ν_9	3121	3187	3261	3230	3239	3153	3159	2885	2991
ν_{10}	1065	1426	1184	1169	1347	1112	1208	1116	1371
ν_{11}	852	903	231	547	1114	1046	1006	696	813
ν_{12}	262	127	**i535 C-Cl antis**	219	217	236	225	210	170

[a] Results of the calculations performed in the present work.

Table 3
Adiabatic (IE_{ad}) and/or vertical (IE_{vert}) ionization energies (eV) for eight cationic states resulting from direct ionization out of the molecular orbitals (MO) calculated at CCSD, M06-2X and/or TDDFT levels in the C_{2h}, C_S and/or C_2 symmetry point groups. The results of previous quantum chemical calculation results [5–7] and [32] are included.

State	$\tilde{X}^2A_u$		$\tilde{A}^2A_g$		$\tilde{B}^2B_u$		$\tilde{C}^2B_g$	
Level	IE_{ad}	IE_{vert}	IE_{ad}	IE_{vert}	IE_{ad}	IE_{vert}	IE_{ad}	IE_{vert}
CCSD (C_{2h})	9.45	9.73	11.92	11.94	12.03	12.07	12.59	12.69
M06-2X (C_{2h})	9.53	9.83	11.87	11.9	12.04	12.08	12.66	12.76
TDDFT (C_S)	9.53	9.83	11.68	11.72	11.83	11.87	12.52	12.62
EHT [5]	-	11.8	-	12.6	-	13.0	-	13.6
OVGF [6]	-	9.50	-	11.66	-	11.88	-	12.52
OVGF [7]	-	9.44	-	11.65	-	11.81	-	12.48
SDCI [32]	9.09	-	11.81	-	11.96	-	12.57	-

State	$\tilde{C}^2B_g$		$\tilde{D}^2A_g$		$\tilde{E}^2A_u$		$\tilde{F}^2A_g$		$\tilde{G}^2B_u$		$\tilde{H}^2B_u$
Symm	C_{2h}	C_S	C_{2h}	C_2	C_{2h}		C_{2h}		C_{2h}		C_{2h}
	IE_{ad}	IE_{ad}	IE_{ad}	IE_{ad}	IE_{ad}	IE_{vert}	IE_{ad}	IE_{vert}	IE_{ad}	IE_{vert}	IE_{vert}
TDDFT	12.52	12.47	13.44	13.32	13.37	13.76	15.49	16.03	15.82	16.12	19.13
EHT [5]	13.6*	-	14.4*	-	-	14.8	-	-	-	15.1	18.7
OVGF [6]	12.52*	-	13.81*	-	-	13.96	-	16.10	-	16.21	19.57
OVGF [7]	12.48*	-	13.77*	-	-	13.94	-	16.38	-	16.21	-

* IE corresponding to vertical ionization energy values.

Table 4

Energy position (eV), assignments and average wavenumbers (cm^{-1}) deduced from the structures observed in the HeI-, NeI-, ArII/ArI-PES and TPES of the $\widetilde{X}\,^2A_u$ band of the trans-1,2-$C_2H_2Cl_2^+$. Conversion factor 1 eV = 8065.545 cm^{-1} [34].

PES			TPES[d]	Assignments	
HeI [a]	NeI[b]	ArII[c]		Assignts.	Energy / Average wavenumber
9.633(4)				**$IE_{ad}(\widetilde{X}^2A_u)$**	
9.680(2)	9.684		9.677(3)	ν_5	$\omega_5 = 0.047 \pm 0.006$ eV
9.729(6)		9.682	9.723(4)	$2\nu_5$	379 ± 50 cm^{-1}
9.759(3)	9.751		9.748(3)	ν_4	$\omega_4 = 0.110 \pm 0.008$ eV
9.777(5)		9.770	9.771(6)	$3\nu_5$	887 ± 60 cm^{-1}
9.808(2)	[9.814]	9.811	9.812(3)	**ν_2**	$\omega_2^{av} = 0.171 \pm 0.005$ eV
9.859(3)	[9.861]	9.849	9.855(2)	$\nu_2+\nu_5$	1379 ± 40 cm^{-1}
9.907(2)	9.916	9.907	9.903(2)	$\nu_2+2\nu_5$	$\omega_{e2}^{ext} = 0.180 \pm 0.004$ eV
			9.928(3)	$\nu_2+\nu_4$	1452 ± 30 cm^{-1}
9.967(2)		9.951	9.949(8)	$\nu_2+3\nu_5$	
9.985(5)	[9.987]	9.985	9.981(3)	**$2\nu_2$**	
10.041(1)	10.038	10.029	10.027(3)	$2\nu_2+\nu_5$	
10.098(5)	10.093	10.098	10.084(3)	$2\nu_2+2\nu_5$	
10.154(2)	[10.160]	10.151	10.155(5)	**$3\nu_2$**	
10.184(1)		10.181	10.190(9)	$3\nu_2+\nu_5$	
10.290(5)	10.270		10.280(5)	$3\nu_2+\nu_4$	
10.339(5)	[10.329]		10.332(4)	**$4\nu_2$**	
	10.376		10.387(3)	$4\nu_2+\nu_5$	
	10.443		10.435(2)	$4\nu_2+\nu_4$	
			10.461(3)	$4\nu_2+2\nu_5$	
	[10.491]		10.484(2)	$4\nu_2+3\nu_5$	
			10.499(5)	**$5\nu_2$**	
	10.538		10.521(3)	na	
	10.577		10.548(2)	$5\nu_2+\nu_5$	
			10.606(2)	$5\nu_2+\nu_4$	
	10.652		10.669(2)	**$6\nu_2$**	
			10.719(5)	$6\nu_2+\nu_5$	
			10.785(4)	$6\nu_2+\nu_4$	
			10.878(4)	$6\nu_2+2\nu_4$	
			10.901(3)	$[7\nu_2+\nu_4]$	
			10.925(3)	$[7\nu_2+3\nu_5]$	
			10.960(5)	na	
			10.998(5)	**$8\nu_2$**	
			11.038(2)	$8\nu_2+\nu_5$	
		[11.079]	11.087(5)	$8\nu_2+2\nu_5$	
			11.119(5)	$8\nu_2+\nu_4/3\nu_5$	
		[11.167]	11.158(3)	**$9\nu_2$**	
			11.245(2)	$9\nu_2+2\nu_5$	
			11.276(4)	$9\nu_2+\nu_4/3\nu_5$	
			11.299(3)	**$10\nu_2$**	
			11.361(3)	$10\nu_2+2\nu_5$	
			11.407(4)	$10\nu_2+\nu_4$	
			11.445(5)	**$11\nu_2$**	
		[11.483]	11.498(5)	$11\nu_2+\nu_5$	
			11.580(5)	$11\nu_2+3\nu_5$	
			11.613(5)	**$12\nu_2$**	
		[11.624]	11.639(5)	na	
			11.678(4)	$12\nu_2+2\nu_5$	

[a] Average position of the structures observed in six HeI-PES recorded with 4 meV energy increments. The largest deviation from the average is mentioned in parentheses.

[b] Average position of the structures observed in two NeI-PES recorded with 4 meV energy increments. The average deviation is about ±0.005 eV. The contribution of the 16.67 eV (74.37 nm) line of the NeI doublet is given in square brackets: the intensity ratio NeI (16.85 eV)/NeI (16.67 eV)≈ 3/1 [20].

[c] Average position of the structures observed in two ArII-PES recorded with 4 meV energy increments. The average deviation is about ±0.005 eV. The structure generated by the ArI-doublet at 11.83/11.67 eV (104.82/106.67 nm) doublet is given in square brackets.

[d] Average position of the structures observed in five TPES recorded with 5 meV energy increments with and without LiF filter. The largest deviation from the average is mentioned in parentheses.

only the vibrational normal modes belonging to the a_g representation should be observed in the spectra.

In the C_{2h} symmetry point group, the $\widetilde{C}\,^2B_g$ ionic state corresponds to a saddle point characterized by an imaginary wave number involving the elongation of the C-Cl bond and the variation of the H-C = C and Cl-C = C angles. In the C_S group, this ionic state shows a true minimum and the corresponding wavenumbers are listed in Table 2.

The $\widetilde{D}\,^2A_g$ ionic state corresponds also to a saddle point in the C_{2h} symmetry point group, with an imaginary frequency associated with C = C and C-Cl bond elongations. In the C_2 symmetry point group, this state shows a minimum corresponding to a twist of the H-C = C-Cl groups around the C = C bond.

An attempt to optimize the $\widetilde{H}\,^2B_u$ state in the C_{2h} symmetry point group has been unsuccessful because the C-Cl bond lengths increase very rapidly already at the beginning of the optimization. This state is likely dissociative. Furthermore several states become very close in energy in this range, preventing the geometry optimization.

The vertical and adiabatic ionization energies calculated at different levels are presented in Table 3 together with the results of previous quantum chemical calculations [5–7,32]. The contour maps of the ionized molecular orbitals (MO) represented in Fig. S2 (see Supplementary material) are calculated at the DFT/M06-2X/aug-cc-pVDZ level

and correspond to a 0.1 a.u. density. The positive and negative parts are colored in green and yellow respectively.

5. DISCUSSION OF THE DATA

5.1. HeI-, NeI- and ArII/ArI-PES of trans-1,2-$C_2H_2Cl_2$ (see Figs. 1–3)

As shown in Figs. 1–3 the main modifications induced by changing the excitation energy of the light source concern essentially the relative intensities of the trans-1,2-$C_2H_2Cl_2^+$ ionic states. This is the case even when taking into account the contribution of the weakest component of the doublet in the Ne resonance line (see section 3.1). The band shape of the $\widetilde{X}\ ^2A_u$ state is strongly modified with respect to the HeI-PES. The (0,0) transition in the $\widetilde{B}\ ^2B_u$ band is much stronger whereas the $\widetilde{C}\ ^2B_g$ band is of about the same relative intensity but shows structures extending over a broader energy range. Only the $\widetilde{A}\ ^2A_g$ band seems to be nearly unaffected. The same observations are valid for the ArII/ArI-PES, at least for the $\widetilde{A}\ ^2A_g$ and $\widetilde{B}\ ^2B_u$ ionic states. This behavior is markedly different from those observed in the two other isomers [1,33].

5.1.1. The $\widetilde{X}^2A_u$- PES Band (see Figs. 1b, 2 b and 3 and Table 4)

The HeI-PES of the $\widetilde{X}^2A_u$ band of trans-1,2-$C_2H_2Cl_2^+$ is observed between 9.633 eV and 10.339 eV. This observation does not markedly change when using the NeI- and ArII/ArI-resonance lines: the cationic ground state is observed up to 10.652 eV and 10.181 eV respectively. This would mean that the width of the Franck-Condon region is barely modified. The relative intensities of the vibrational transitions are only slightly affected.

When averaged over the measurements with the HeI-, NeI- and ArII-lines, the adiabatic ionization energy $IE_{ad}(\widetilde{X}^2A_u$, trans-1,2-$C_2H_2Cl_2^+)$ is equal to 9.633 ± 0.004 eV where the indicated uncertainty is given by the largest deviation from the average. In the HeI-PES the transitions at 9.633 eV and at 9.859 eV are of about the same intensity (see Fig. 1b). Table 1 shows that the value of IE_{ad} is in good agreement with the results reported earlier [2,3] ranging from 9.64-9.69 eV. More recently, Woo et al. [30] and Bae et al. [31] using pulsed field ionization photoelectron spectroscopy (PFI-PES) and mass-analyzed threshold ionization (MATI) respectively, determined IE_{ad} $(\widetilde{X}^2A_u)$ at 9.63097 ± 0.00025 eV and 9.6306 ± 0.0006 eV.

Two weak bands are observed at 9.594 eV and 9.543 eV, i.e. at 0.039 eV and 0.090 eV below the adiabatic ionization energy. With respect to the adiabatic transition intensity to the $\widetilde{X}^2A_u$ at 9.633 eV, their intensity ratio is 15% and 8% respectively. These signals are assigned to ν_5 and $2\nu_5$ hot bands ($\omega_5 = 340$ cm^{-1}) for which a relative population of 19% and 4% respectively is calculated at 298 K. This value is in good agreement with $\omega_5 = 350$ cm^{-1} observed in the neutral molecule [29].

The ionization energies reported earlier at about 9.8 eV [2–5] likely correspond to the $IE_{vert} = 9.859 \pm 0.006$ eV measured in the HeI-PES in the present work. Apart from $IE_{ad} = 9.09$ eV reported by Takeshita [32] and $IE_{vert} = 9.29$ eV [5] the calculated values listed in Table 3 are in good agreement with the present experimental measurements and with those reported earlier [2–6].

The energy positions of the structures observed in the first PES band are listed in Table 4. Considering only the results obtained with the HeI resonance line the structures and assignments are listed in columns 1 and 5. The strongest vibrational progression is made of 5 quanta.

For the same progression in the NeI-PES, good agreement is found with the data obtained by HeI-PES. However, the intensity distribution of the vibrational transitions is quite different. In the NeI-PES the equality of the intensity at IE_{ad} and IE_{vert} no longer holds: clearly at $IE_{vert} = 9.814$ eV the transition is much stronger. Only a small part of the intensity difference has to be assigned to the contribution of the NeI-16.67 eV resonance line. The other part has likely to be ascribed to a difference of the Franck-Condon overlap between the intermediate neutral excited state and the ionized final state.

Likely owing to the low signal/noise ratio, in the ArII/ArI-PES the considered progression is only observed up to $v = 3$.

From these results an average spacing of 0.171 ± 0.005 eV ($1\,379 \pm 40$ cm^{-1}) is obtained for the strongest progression. This wavenumber is lower than that reported by Woo et al. [30] of 1452 cm^{-1} and by Bae et al. [31] of 1451 cm^{-1}. The value predicted by quantum chemical calculations in the present work is 1513 cm^{-1} which has to be compared with earlier reported quantum chemical results of 1491 cm^{-1} [30] and 1466 cm^{-1} [31]. Taking anharmonicity into account, a wavenumber of 1454 cm^{-1} is calculated by Woo et al. [30]. By HeI-PES Lake and Thompson [2], Jonathan et al. [3] and Wittel and Bock [4] reported 1410 cm^{-1}, 1230 cm^{-1} and 1400 cm^{-1} respectively.

This wavenumber has unambiguously to be assigned to ν_2, i.e. the C = C stretching vibrational normal mode of a_g symmetry. This assignment is consistent with the characteristics of the ionized $2a_u$ MO with π character.

The first PES band shows at least two other vibrational progressions. Considering the three PES spectra, the strongest of these transitions is characterized by an average wavenumber $\omega = 379 \pm 50$ cm^{-1} (0.047 ± 0.006 eV). This value fits the wavenumber of the ν_5 vibrational mode (C-Cl stretching) predicted at 372 cm^{-1} in the present work. Wavenumbers of 365 cm^{-1} and 368 cm^{-1} are measured for the trans-1,2-$C_2H_2Cl_2^+$ cation in its ground state by using PFI-PES [30] and MATI [31]. This is also in good agreement with the HeI-PES values of 360 cm^{-1} reported by Lake and Thompson [2], of about 400 cm^{-1} and 320 cm^{-1} measured by Jonathan et al. [3] and Wittel and Bock [4] respectively.

A third but weaker vibrational transition is observed and characterized by $\omega = 887 \pm 60$ cm^{-1} (0.110 ± 0.008 eV). This wavenumber may correspond to the ν_4 vibration (CC-H bending motion) for which a wavenumber of 971 cm^{-1} is calculated and observed at 944 cm^{-1} by PFI-PES [30] and at 943 cm^{-1} by MATI [31].

These assignments are fully compatible with the MO ionized at this energy. As shown in Table S1 (bold print) during the ionization of the $2a_u$ MO the C = C bond length is significantly increased whereas the C-Cl internuclear distance is considerably shortened. These geometrical modifications will affect the normal modes involving the C = C and C-Cl stretching coordinates.

5.1.2. The $\widetilde{A}^2A_g$, $\widetilde{B}\ ^2B_u$ and $\widetilde{C}\ ^2B_g$ PES Bands (see Figs. 1b, 2b and 3 and Table S2)

The HeI-, NeI- and ArII/ArI-PES of trans-1,2-$C_2H_2Cl_2$ all show a group of three narrow, well separated PE bands within the energy range extending between 11.8 eV and 13 eV. Comparing to the HeI-PES, the relative intensity of the first two bands in the NeI-PES is inverted whereas the last resolved band has about the same intensity but shows a broadening toward higher energies. The intensity of the first two bands dominates the ArII/ArI-PES. It has to be mentioned that the ArI resonance line at 11.83 eV (95417.6 cm^{-1}) is nearly resonant with $IE_{ad}(\widetilde{A}^2A_g) = 11.84$ eV generating nearly zero kinetic energy electrons.

The first PE band of this group corresponds to the ionization of the $5a_g$ MO (see Fig. S2). Its IE_{ad} is predicted between 11.68 eV and 11.91 eV in this work or at 11.81 eV [32] depending on the calculation level. The measured value averaged over the three PES is $IE_{ad}(\widetilde{A}^2A_g) = IE_{vert} = 11.840 \pm 0.008$ eV. This value agrees well with previously reported results [2–6].

This band shows two very short vibrational progressions: two quanta of ν_4 and a single quantum ν_5 combined with ν_4. Averaged values for $\omega_4 = 605 \pm 30$ cm^{-1} (0.075 ± 0.004 eV) and for $\omega_5 \approx 320$ cm^{-1} (0.040 eV) are measured. These wavenumbers have to be compared with the values of 676 cm^{-1} and 305 cm^{-1} respectively predicted in the present work. Takeshita [32] calculated $\omega_4 = 723$ cm^{-1} and $\omega_5 = 324$ cm^{-1}. These values correspond to vibrations involving Cl-C-C and H-C-Cl bending and C-Cl stretching motions respectively. Only Wittel and Bock [4]

reported a wavenumber of 600 cm^{-1} for the band at 11.82 eV. Lake and Thompson [2] assigned a structure observed at 11.93 eV to the ionization of a b_g non-bonding orbital. In the present work this structure is assigned to the vibrational excitation (ν_4 at 11.919 eV or $\nu_4+\nu_5$ at 11.953 eV) of the $\widetilde{A}\,^2A_g$ state (see Table S2 in Supplementary Material).

The ionized n(Cl) MO has an antibonding C-Cl and bonding C-H character. From this situation a decrease in the C-Cl distance and an increase of C-H bond length should result. These changes will induce the excitation of the above-mentioned vibrational motions.

The second band of this group corresponds to an adiabatic ionization energy, $IE_{ad} = 12.044 \pm 0.005$ eV. This value has to be compared with 11.93 eV [2] and with 12.01-12.1 eV [3–6] reported in earlier papers. Quantum chemical calculations predict $IE_{ad} = 11.83$-12.04 eV for the ionization of the $4b_u$ MO of trans-1,2-$C_2H_2Cl_2$. The ionized MO is a Cl-Cl bonding combination of n(Cl) MOs. The molecular parameters are the same as those involved in the first excited $\widetilde{A}\,^2A_g$ state, but with opposite effects. The resulting $\widetilde{B}\,^2B_u$ state shows a slightly lengthened C-Cl distance and strongly modified H-C-C and Cl-C-C angles. As excited by the NeI- and ArII/ArI-resonance lines the adiabatic and vertical ionization energies are equal. The intensity distribution profile of the vibrational structure is quite similar.

From the analysis of this band a short vibrational progression is observed with a wavenumber of 740 ± 40 cm^{-1} (0.092 ± 0.005 eV) (see Table S2). Jonathan et al. [3] reported an approximately constant separation of about 0.080 eV or 645 cm^{-1}. Wittel and Bock [4] reported a wavenumber of 640 cm^{-1} for the PES band at 12.01 eV. The wavenumber of 740 ± 40 cm^{-1} is best fitted by the calculated wavenumbers of $\omega_4 = 821$ cm^{-1} (of a_g symmetry) or $\omega_8 = 772$ cm^{-1} (of b_g symmetry), both involving the C-H bending motion. Takeshita [32] calculated $\omega_4 = 856$ cm^{-1}. Excitation of ν_8 is, however, symmetry forbidden and therefore less probable, even if its wavenumber better fits the experimental data.

Combined with ν_4 a lower wavenumber is detected at 516 ± 20 cm^{-1} (0.064 ± 0.005 eV)(see Table S2). By quantum chemical calculations this observed wavenumber is only consistent with $\omega_{11} = 564$ cm^{-1} of b_u symmetry. This vibration involves both anti-symmetric C-Cl stretch and C-H bending. Excitation of this motion is symmetry-forbidden. However, the $\widetilde{B}\,^2B_u$ state and the very closely lying $\widetilde{C}\,^2B_g$ could couple and lead to a symmetry lowering because the equilibrium geometry of the $\widetilde{C}$ state corresponds to the C_s symmetry (see section 4.2). A symmetry-forbidden b_u mode in C_{2h} correlates to a symmetry-allowed a' mode in the C_s symmetry point group.

Concerning the intensity, the third band of this group is the less altered by changing the excitation energy of the light source. In the HeI- and ArI/ArII-PES it clearly shows a threshold at $IE_{ad} = IE_{vert} = 12.582 \pm 0.006$ eV but in the NeI-PES $E_{vert} = 12.789 \pm 0.004$ eV. Compared to previous determinations, the present measurements satisfactorily agree with IE_{vert} ranging from 12.55 eV to 12.66 eV [2–4]. These IE's should be assigned to the ionization of the $1b_g$ MO which has its predicted $IE_{ad} = 12.32$ eV and $IE_{vert} = 12.49$ eV. It involves a considerable lengthening of the C-Cl internuclear distance and strong H-C-C and Cl-C-C angular alterations. In the C_{2h} symmetry point group the optimized geometry of this state is a saddle point characterized by an imaginary ν_{12} wavenumber. In the C_S symmetry point group, however, geometry optimization of this ionized state (becoming $\widetilde{C}\,^2A''$) leads to a true minimum.

The analysis of this band in the HeI- and NeI-PES reveals a first dominating progression of four (in HeI-PES) to six (in NeI-PES) vibrational levels with 839 ± 30 cm^{-1} (0.104 ± 0.004 eV) separation (see Table S2). This wavenumber has to be compared with the computed values of ω_4 (785 cm^{-1} in the C_{2h} point group and 843 cm^{-1} in the C_s point group) for the totally symmetric ν_4 vibrational mode which involves the C-Cl stretching. Takeshita [32] calculated this wavenumber at 850 cm^{-1}. Lake and Thompson [2] reported 770 cm^{-1} assigned to the C-Cl stretching. Wittel and Bock [4] measured 720 cm^{-1}. Jonathan et al. [3] reported a tentative value of 720 cm^{-1}.

In the HeI-PES, a second vibrational mode appears in combination with ν_4 for which a separation of 314 ± 60 cm^{-1} (0.039 ± 0.007 eV) is measured. This energy interval can be assigned to the computed wavenumber $\omega_5 = 334$ cm^{-1} (C_{2h} point group) or 286 cm^{-1} (C_s point group) involving a totally symmetric C-Cl bending vibration.

In Table S2 it has explicitly been noticed that an alternative assignment is possible for ν_4. An interval $\omega_x = 660 \pm 50$ cm^{-1} (0.082 ± 0.006 eV) could be the alternative and correspond to the ν_8 vibrational motion (a" symmetry) in the C_S symmetry point group.

5.1.3. *The $\widetilde{D}\,^2A_g$- $\widetilde{E}\,^2A_u$ PES Bands (see Figs. 1a, 2a and Table S3a)*

The fifth PES band only observed with the HeI- and the NeI-resonance lines is spread over 13.5-15.5 eV and is shown in Fig.1a and 2a. Its shape clearly indicates that this band is consisting of two overlapping electronic states. Both exhibit a regular structure.

The lowest energetic component of this band has its IE_{ad} at 13.581 ± 0.005 eV and its IE_{vert} at 13.770 eV in the HeI-PES. This IE is considerably shifted to 14.008 eV in the NeI- PES. Jonathan et al. [3] measured $IE_{ad} = 13.59$ eV whereas the IE_{vert} ranges from 13.88 eV to 13.91 eV [2–6]. These IE values are assigned to the $\widetilde{D}\,^2A_g$ ionic state corresponding to the ionization of the $4a_g$ MO for which $IE_{ad} = 13.32$ eV and $IE_{vert} = 13.44$ eV are predicted. In the C_{2h} symmetry point group, the optimized geometry of the $\widetilde{D}\,^2A_g$ state is a saddle point with ν_7 being an imaginary wavenumber. During the transition to this state the major geometrical modification is the noticeable lengthening of both the C-Cl and the C = C internuclear distances, as can be easily understood based on the MO shape in Figure S2. The H-C-C and Cl-C-C angles remain almost unchanged. The potential energy surface of this state has a true minimum in the C_2 symmetry point group becoming $\widetilde{D}\,^2A$ with only C-Cl bond lengthening and an H-C-C angular opening. The molecule is no longer planar.

As shown in Table S3a (see Supplementary Material) the vibrational analysis of this band is not unambiguous. From the best resolved HeI-PES the most straightforward analysis provides the largest wavenumber $\omega_x' = 1726 \pm 50$ cm^{-1} (0.214 ± 0.006 eV). It best fits $\nu_2 = 1683$ cm^{-1} predicted by the calculations of the present work. This vibration would be combined with $\omega_y' = 258 \pm 40$ cm^{-1} (0.032 ± 0.005 eV) corresponding to the molecular bending wavenumber 321 cm^{-1} calculated for ν_5. This assignment is valid in the frame of the C_{2h} symmetry point group.

Alternatively, the same progression could be decomposed into three wavenumbers. In this choice the ν_5 vibration is maintained. The ω_x' would consist of $\omega_x = 1024 \pm 50$ cm^{-1} (0.127 ± 0.006 eV) and $\omega_y = 734 \pm 40$ cm^{-1} (0.091 ± 0.005 eV). These three experimental values are compatible with those predicted at 1009 cm^{-1}, 729 cm^{-1} and 317 cm^{-1} for ν_3, ν_4 and ν_5 respectively as calculated in the frame of the C_2 symmetry point group. On the basis of the intensity distribution in the PES band the last assignment could be more probable.

As shown in Fig. 1a a sudden intensity increase is detected up from 14.081 ± 0.006 eV and considered as $IE_{ad} = IE_{vert}(\widetilde{E}\,^2A_g)$. This result agrees with earlier determinations lying at 13.96 eV [2–5]. The intensity regularly decreases for the energy increasing up to 14.394 eV in the HeI-PES. The same band extends up to 14.685 eV in the NeI-PES. These latter data will be discussed in the forthcoming section 5.2.

By quantum chemical calculations IE_{vert} values are predicted in the 13.76-13.94 eV range in references [5–7] and in the present work. The $1a_u$ MO is involved and its ionization brings about strong changes of bond lengths (C-Cl, C-H) and angles (H-C-C, Cl-C-C) in the molecule.

The fairly extended progression seems to consist of one vibrational motion, i.e. $\omega_5 = 290 \pm 60$ cm^{-1} (0.036 ± 0.007 eV) (see Table S3a). This value agrees with the value calculated for ν_5 at 296 cm^{-1}. This vibration is expected to be excited considering the geometrical modifications involved during this transition.

5.1.4. The $\widetilde{F}\ ^2A_g$- $\widetilde{G}\ ^2B_u$ and $\widetilde{H}\ ^2B_u$-PES Bands (see Figs. 1a, 2 a and Table S4)

The seventh PES band spreads between 15.7 eV and 16.8 eV but shows two distinguishable vibrational structures. The lowest IE as averaged over the HeI- and NeI-PES is $IE_{ad} = 15.725 \pm 0.004$ eV and $IE_{vert} = 16.139 \pm 0.006$ eV. These results have to be compared to $IE_{ad} = 15.62$ eV [3] and IE_{vert} ranging from 16.19 eV [4] to 16.23 eV [2, 5,6]. By quantum chemical calculations $IE_{ad} = 15.49$ eV and $IE_{vert} = 16.03$ eV have been obtained for the $3a_g$ MO ionization in good agreement with the experimental determinations.

The equilibrium geometry of the $\widetilde{F}\ ^2A_g$ state in the C_{2h} symmetry point group of trans-1,2-$C_2H_2Cl_2^+$ has been calculated. The most affected molecular parameters on the $3a_g$ MO ionization is the increase of C = C and C-H bond lengths. The H-C-C and Cl-C-C bond angles are considerably decreased. The wavenumbers calculated for the vibrational normal modes in the $\widetilde{F}\ ^2A_g$ state are listed in Table 2.

From the data listed in Table S4 (see Supplementary Material) a fairly long vibrational progression is observed with a spacing of 0.105 ± 0.006 eV (847 ± 50 cm^{-1}). Only Wittel and Bock [4] reported a vibrational wave number of 880 cm^{-1} in good agreement with the present determination but did not assign it. The wavenumber of 847 ± 50 cm^{-1} best agrees with the predicted $\omega_4 = 813$ cm^{-1} assigned to the H-C-C bending vibration and consistent with the large H-C-C bond angle variation during the transition. Combined with ν_4 a weaker structure regularly appears at an average separation of 363 ± 80 cm^{-1} (0.045 ± 0.010 eV). This value could reasonably only be compared to the predicted $\omega_5 = 347$ cm^{-1} assigned to the ν_5 C-Cl stretch and H-C-C bending vibration.

The sudden intensity variation in the vibrational progression at 16.325 eV is ambiguous: it could be assigned to (i) the $6\nu_4$ excitation within the $\widetilde{F}\ ^2A_g$ band or (ii) the IE_{ad} of the next $\widetilde{G}\ ^2B_u$ state. However, based on its intensity, the latter assignment is favored. By quantum chemical calculations, $IE_{ad} = 15.82$ eV and $IE_{vert} = 16.21$ eV have been obtained. The same calculations show that the $3b_u$ MO ionization leads to a strong H-C-C angular closing and moderate C-Cl and C = C bond lengthening.

Starting from 16.325 eV a vibrational progression is observed with $\omega_i = 645 \pm 50$ cm^{-1} (0.080 ± 0.006 eV). This wavenumber is close to both 716 cm^{-1} and 691 cm^{-1} predicted for ν_4 and ν_8 respectively. Both vibrational motions involve H-CC bending (see Fig. S1) but only ν_4 is symmetry-allowed.

Well isolated in the spectrum the last $\widetilde{H}\ ^2B_u$ HeI-PES band is very weak and has $IE_{ad} = 19.00$ eV. Weaker broad shoulders are observed near 19.33 eV and 19.64 eV. The broadness of the structure could be related to the predicted dissociative character of the $\widetilde{H}\ ^2B_u$ state as mentioned earlier (see section 4.2).

5.2. Threshold PES of trans-1,2-$C_2H_2Cl_2$ (see Figs. 4 and 6, Tables 4 and S2-S4)

The TPES observed in this work is reproduced in Fig. 4a between 9.5 eV and 20.5 eV and compared to the HeI-PES normalized to the adiabatic transition to the ionic ground state. In spite of the higher resolution achieved in the TPES (about 4 meV) very few structures are resolved. In Fig. 4b the low energy region between 9.5 eV and 13.5 eV has been reproduced on an extended energy scale. To avoid second order light contributions, the 9.5-11.8 eV energy range has been recorded introducing a LiF window on the light path (see Fig.6a). The energy position of the features observed in the $\widetilde{X}^2A_u$-PES band is listed in Table 4. Up to 10.332 eV the agreement with the HeI-PES is satisfactory. The Δ-plot of the TPES of the $\widetilde{X}^2A_u$ state and of the PAS of trans-1,2-$C_2H_2Cl_2$ [21] in the same energy range is reproduced in Fig.6b. Particularly above 10.2 eV this comparison very convincingly shows in detail the fate of the successively involved Rydberg states generating

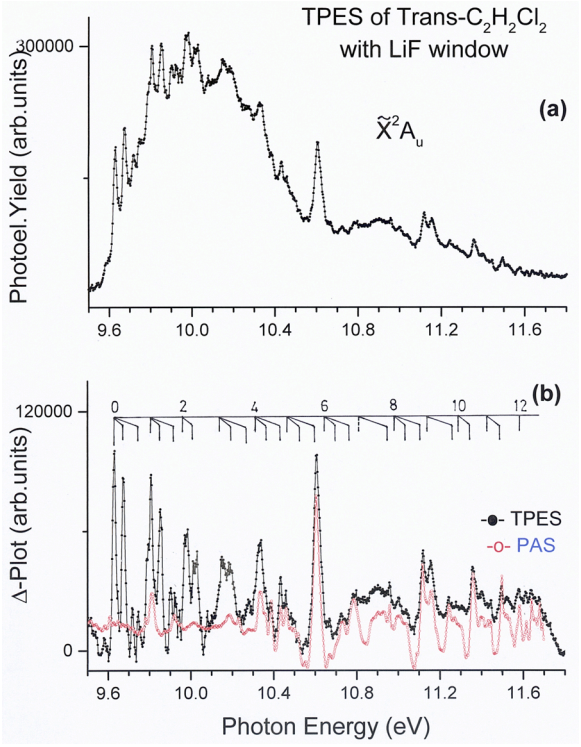

Fig. 6. (a) TPES of the $\widetilde{X}\ ^2A_u$ state of trans-1,2-$C_2H_2Cl_2^+$ on an extended photon energy scale recorded with a LiF window (cutoff at 11.8 eV). (b) Δ-plot of the TPES (black curve) and PAS (red curve) [21] of trans-1,2-$C_2H_2Cl_2$ in the same energy range. Vertical bars show the main vibrational structure.

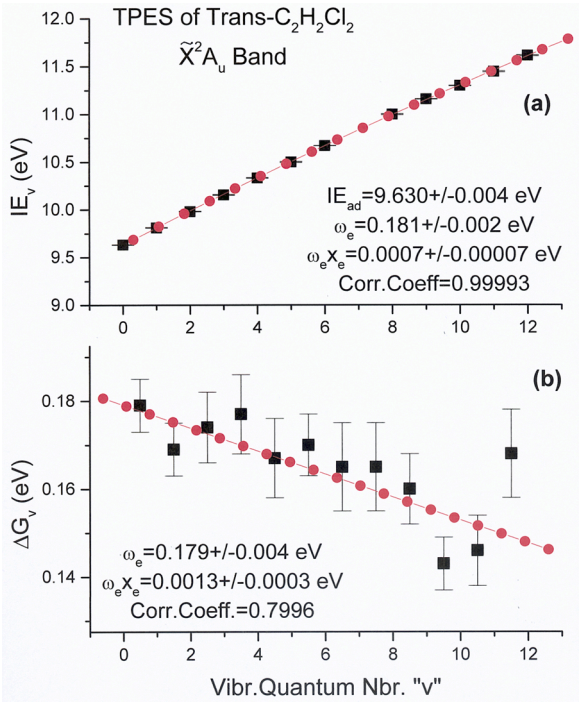

Fig. 7. (a) IE_v-vs-v plot for the $\widetilde{X}\ ^2A_u$ TPES band of trans-1,2-$C_2H_2Cl_2^+$: the red line represents the least square fitting by a polynomial fit and the derived quantities are inserted. (b) ΔG_v-vs-v plot for the same ionic state: the red line represents the least square fitting and the derived quantities are inserted.

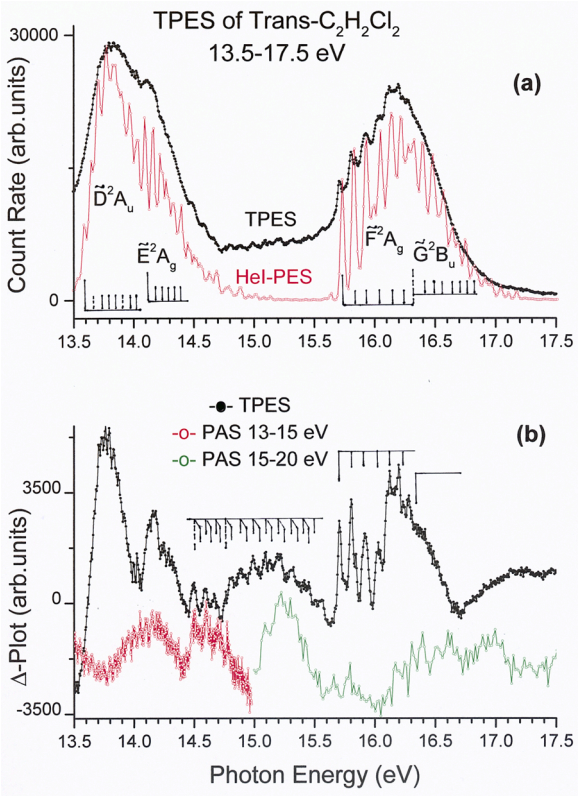

Fig. 8. (a) TPES (black line) and HeI-PES (red line) of trans-1,2-$C_2H_2Cl_2$ between 13.5 eV and 17.5 eV. Vertical bars indicate the main vibrational structure. (b) Δ-plot of the TPES (black curve) and PAS [21] (red and green curves) in the same photon energy range. Vertical bars indicate the main vibrational structure.

zero-kinetic-energy electrons through resonant autoionization. The energy position of the extended ν_2 vibrational progression observed in the TPES and the NeI-PES are inserted in Table 4. The correlation between PAS, TPES and NeI-PES is clear.

The measurement of the TPES of the $\widetilde{X}^2A_u$ state allowed us to observe the main ν_2 vibrational progression up to v = 12. In Fig. 7a the energy positions were plotted as a function of the vibrational quantum number v. The least square fit provides the parameters shown in the same figure. A correlation coefficient of 0.99993 is obtained. By this way an anharmonic $\omega_{e2} = 1460 \pm 16\ cm^{-1}$ (0.181 ± 0.002 eV) is obtained. This value has to be compared to the average value of $1379 \pm 40\ cm^{-1}$ obtained from the HeI-PES (see section 5.1.1.) and with the most recent and accurate wavenumbers of 1451 cm^{-1} [30] and 1452 cm^{-1} [31]. Using the $\Delta G_v(v)$-plot in Fig. 7b a similar value $\omega_{e2} = 1444 \pm 30\ cm^{-1}$ (0.179 ± 0.004 eV) is obtained.

The energy positions corresponding to the structure in the $\widetilde{A}^2A_g$, $\widetilde{B}\ ^2B_u$, $\widetilde{C}\ ^2B_g$, $\widetilde{D}\ ^2A_g$- $\widetilde{E}\ ^2A_u$ and the $\widetilde{F}\ ^2A_g$- $\widetilde{G}\ ^2B_u$ TPES bands are listed in Tables S2-S4 together with their assignments. However, in the energy range corresponding to the two latter PES bands, $\widetilde{D}\ ^2A_g$- $\widetilde{E}\ ^2A_u$ and $\widetilde{F}\ ^2A_g$- $\widetilde{G}\ ^2B_u$, the shape of the HeI-PES and TPES bands markedly differs as illustrated in Fig. 8a. For more clarity the corresponding Δ-plot is displayed in Fig. 8b showing the abundant structure generated by threshold photoelectrons. In the same figure, the Δ-plot of the PAS of trans-1,2-$C_2H_2Cl_2$ [21] in the same photon energy range has been inserted. The close correlation is obvious. The energy position of these structures is listed in Table S3b. Three salient features have to be stressed.

First, the observation in the TPES of $IE_{ad} = 14.087$ eV ($\widetilde{E}\ ^2A_g$ band) has to be mentioned confirming the value of 14.081 eV measured in the HeI-PES. Second, the $IE_{ad} = 16.325$ eV in the HeI-PES corresponds to the starting point at 16.332 eV of a band considered as a continuum in the TPES. A sudden intensity increase in the vibrational structure of the $\widetilde{F}\ ^2A_g$ ionic state coincides with an increase of absorption in the PAS [21].

The last and most salient feature in this energy range of the TPES is the abundant structure observed in the Franck-Condon gap between the $\widetilde{E}\ ^2A_u$ and $\widetilde{F}\ ^2A_g$ cationic states and analyzed in Table S3b. With the help of the PAS [21] this series of signals has been partitioned into two parts: (i) a short progression starting at $IE_1 = 14.495$ eV clearly corresponding to a PAS band arising at the same energy and (ii) a longer progression starting at $IE_2 = 14.794$ eV. In both series similar wavenumbers are observed for the main progression, i.e. $\omega_X = 734 \pm 50\ cm^{-1}$ (0.090 ± 0.006 eV) and $\omega_A = 831 \pm 50\ cm^{-1}$ (0.103 ± 0.006 eV). Both appear combined with $\omega_Y = \omega_B = 280 \pm 30\ cm^{-1}$ (0.035 ± 0.004 eV) which also fits the wavenumber of $290 \pm 60\ cm^{-1}$ (0.036 ± 0.007 eV) measured for the $\widetilde{E}\ ^2A_u$ state as observed in the HeI-PES. It is difficult to decide whether the observed structures belong to one unique or to two successive progressions. This or these sequences could be assigned to autoionizing transitions from the successive vibrational levels of the intermediate neutral Rydberg states to the $\widetilde{E}\ ^2A_u$ ionization continuum. These Rydberg states belong to series converging to the $\widetilde{F}\ ^2A_g$- $\widetilde{G}\ ^2B_u$ ionization continua.

Above 17.5 eV photon energy, beside the weak band at 19.00 eV assigned to the $\widetilde{H}\ ^2B_u$ state a very weak photoelectron band is observed with a maximum at about 18.00 eV. This additional TPES band corresponds to an absorption band in the PAS [21].

5.3. *The CIS spectra (see Fig. 5)*

The CIS spectra of the $\widetilde{X}\ ^2A_u$ and $\widetilde{A}^2bA_g$ ionic states have been measured over 8 eV and are displayed in Fig. 5a. The Δ-plot of the vacuum UV PAS in the 12-17 eV energy range has been included [21].

At the opposite of previous observations [1,33] the shape of the CIS spectra of trans-1,2-$C_2H_2Cl_2^+$ appears to be more state-specific. In Fig. 5a three vibrational states of the $\widetilde{X}\ ^2A_u$ electronic state, i.e. $\nu_2 = 0$, 4 and 9, show quite different CIS curves above 12 eV photon energy. This indicates that different neutral Rydberg states are involved each leading specifically to an individual vibronic state through autoionization. The same figure displays the CIS curve related to the (0,0)-transition of the $\widetilde{A}^2A_g$ state which also shows large differences in the same photon energy range.

Contrary to the high energy range, near threshold vibrationally resolved CIS spectra were recorded for $\nu_2 = 0$-10 and are shown in Fig. 5b. An abundant structure is observed between the onsets and 12 eV. The Δ-plot of the vacuum UV PAS has been reproduced between 9.5 eV and 12 eV [21]. All Rydberg states identified in this region are involved in the population of the successive vibrational levels of the $\widetilde{X}\ ^2A_u$ state of trans-1,2-$C_2H_2Cl_2^+$.

More or less important alterations of the relative intensities within a PES-band in the NeI- and ArII-PES have been stressed in section 5.1. Beside the contribution ascribed to the NeI-16.67 eV or the ArI-11.83 eV resonance lines an additional part has to be assigned to the autoionization of well defined Rydberg states as clearly identified by CIS spectroscopy.

6. Conclusions

The HeI-, NeI-, and ArII/ArI-PES of trans-1,2-$C_2H_2Cl_2$ have been measured in the laboratory. The TPES and CIS spectra have been recorded using synchrotron radiation. Nine PES bands have been detected between the lowest IE_{ad} at 9.633 eV and 21 eV. The assignments of these bands and their vibrational structure were based on quantum chemical calculations. The reliability of the assignments is based on the good correlation between the theoretical predictions and the experimental values. The TPES and CIS spectra show the significant

Table 5
Comparison of the adiabatic (IE_{ad}) and vertical (IE_{vert}) ionization energies (eV) measured in the three $C_2H_2Cl_2$ isomers using HeI-PES. Asterisks indicates those ionic states for which $IE_{ad} = IE_{vert}$.

States		$\widetilde{X}$	$\widetilde{A}$	$\widetilde{B}$	$\widetilde{C}$	$\widetilde{D}$-$\widetilde{E}$		$\widetilde{F}$-$\widetilde{G}$		$\widetilde{H}$
IE_{ad}	1,1-	9.828	11.520	12.157*	12.497	13.521	-	15.539	-	18.496*
	Cis-[a]	9.666	11.426	11.965	12.375	13.592	-	15.531	16.638	-
	Trans-	9.633	11.840*	12.044*	12.582*	13.581	14.081	15.724	16.325	19.00*
IE_{vert}	1,1-	9.992	11.647	12.157*	12.536	13.633	14.195	-	-	18.496*
	Cis-[a]	9.844	11.690	12.028	12.460	13.748	14.083	15.684	16.815	18.80
	Trans-	9.856	11.840*	12.044*	12.582*	13.774	14.169	16.139	16.482	19.00*

[a] Ref. [33]: R. Locht, D. Dehareng, B. Leyh, *unpublished results.*

autoionization contribution of well identified Rydberg states [21] to the relative intensity changes of the successive electronic (vibrational) states.

After a detailed investigation of the three $C_2H_2Cl_2$ isomers a few qualitative observations are noteworthy. The fixed wavelength PES (HeI-, NeI-, ArII-) of the 1,1- [1] and cis-1,2-isomers [33] exhibit very large differences whereas the trans-1,2-isomer is just slightly perturbed by changing the excitation light source. The HeI-PES of the trans-isomer is dominated by the ionization of the 3p-Cl lone pair orbitals. By contrast, these bands are of about the same intensity as the ground state in the two other isomers [1,33]. The TPES of the three isomers are very similar above 13 eV. Below this energy the three isomers exhibit major differences, particularly in the energy region of the ground state of the ion.

Quantitatively the (T)PES spectra show several marked trends (see Table 5): (i) the adiabatic IE increases in the sequence trans-≤cis-<1,1-isomer for the ground state $\widetilde{X}$ of the molecular ion : the C = C π orbital is predominantly involved. (ii) The adiabatic IE increases in the sequence cis-<1,1-<trans-isomer for the $\widetilde{X}$, $\widetilde{C}$, $\widetilde{F}$ and $\widetilde{H}$ ionic states. For the $\widetilde{B}$ state, the order 1,1- and trans- is inverted. The non-bonding lone pair orbitals of the Cl atoms are implied. Their character is most obvious in the trans-isomer where only the IE_{ad} is observed for the $\widetilde{A}$, $\widetilde{B}$ and $\widetilde{C}$ states with a very short vibrational progression. (iii) The $\widetilde{D}$ - $\widetilde{E}$ bands overlap in the spectra of the three isomers whereas the $\widetilde{F}$ - $\widetilde{G}$ bands only overlap in the 1,1 and 1,2-trans isomers. These states mostly involve σ C-Cl orbitals.

Our calculations indicate that a coupling between the $\widetilde{B}\,^2B_u$ state and the closely lying $\widetilde{C}\,^2B_g$ state should take place. A comparable situation has been observed earlier in the cis-1,2-$C_2H_2Cl_2$ PES [35]. The comparison between experimental and simulated PES spectra including vibronic coupling, such as those presented earlier for cis-1,2-$C_2H_2Cl_2$ [35], would be necessary to evaluate if non-adiabatic effects affect significantly the spectra. This comment is also valid for the $\widetilde{D}$ - $\widetilde{E}$ doublet band where the description of the dynamics might be even more complicated. The fact that no strong irregular patterns have been identified and that the zero-order analysis fits reasonably well the experimental data suggests, however, that these couplings may remain reasonable.

Acknowledgments

We are indebted to the University of Liège for financial support. R.L. and B.L. gratefully acknowledge the European Community for its support through its TMR (Contract EU-HPRI-1999CT-00028) and I3 (Contract R II 3 CT-2004-506008) programmes. D.D.'s contribution was supported by the Belgian program on Interuniversity Attraction Poles of the Belgian Science Policy (IAP n° P6/19).

Appendix A. Supplementary data

Supplementary material related to this article can be found, in the online version, at doi:https://doi.org/10.1016/j.elspec.2020.147033.

References

[1] R. Locht, D. Dehareng, B. Leyh, J. Phys. Commun 1 (2017) 055030.
[2] R.F. Lake, H. Thompson, Proc. Roy. Soc. London A 315 (1970) 323.
[3] N. Jonathan, K. Ross, V. Tomlinson, Intern. J. Mass Spectrom. Ion Phys. 4 (1970) 51.
[4] (a) K. Wittel, H. Bock, Chem. Ber. 107 (1974) 317;
(b) H. Bock, K. Wittel, J. Chem. Soc Chem. Comm. 602 (1972).
[5] A. Berndtsson, E. Basilier, U. Gelius, J. Hedman, M. Klasson, R. Nilsson, C. Nordling, S. Svensson, Phys. Scripta 12 (1975) 235.
[6] W. Von Niessen, L. Åsbrink, G. Bieri, J.Electr. Spectry. Rel.Phenom. 26 (1982) 173.
[7] M.A. Parkes, S. Ali, C.R. Howle, R.P. Tuckett, A.E.R. Malins, Mol. Phys. 105 (2007) 907.
[8] Ch. Servais, R. Locht, Chem. Phys.Letters 236 (1995) 96.
[9] R. Locht, B. Leyh, K. Hottmann, H. Baumgärtel, Chem. Phys. 220 (1997) 217.
[10] I. Lindau, J.C. Helmer, J. Uebbing, Rev. Sci. Instrum. 44 (1973) 265.
[11] (a) R. Locht, B. Leyh, W. Denzer, G. Hagenow, H. Baumgärtel, Chem.Phys. 155 (1991) 407;
(b) R. Locht, B. Leyh, D. Dehareng, K. Hottmann, H. Baumgärtel, J. Phys. B 43 (2010) 015102;
(c) R. Locht, D. Dehareng, B. Leyh, Mol. Phys. 112 (2014) 1520.
[12] (a) R. Carbonneau, E. Bolduc, P. Marmet, Can. J. Phys. 51 (1973) 505;
(b) R. Carbonneau, P. Marmet, Can. J. Phys. 51 (1973) 2202;
(c)ibid. Phys.Rev.A 9 (1974) 1898 and references therein.
[13] L. Moore, Brit. J. Appl. Phys. (J.Phys.D) 1 (1968) 237.
[14] A.F. Carley, R.W. Joyner, J. Electr. Spectrom. Rel. Phenom. 16 (1979) 1.
[15] J.D. Allen, F.A. Grimm, Chem. Phys. Letters 66 (1979) 72.
[16] S. Goursaud, R. Abouaf, Intern. J. Mass Spectrom. Ion Phys. 40 (1981) 351.
[17] R. Locht, G. Caprace, J. Momigny, Chem. Phys.Letters 111 (1984) 560.
[18] R. Locht, D. Dehareng, B. Leyh, J. Phys. B 45 (2012) 115101.
[19] R. Locht, D. Dehareng, B. Leyh, J. Phys. B 47 (2014) 085101.
[20] R. Gorden, R.E. Rebbert, P. Ausloos, Rare Gas Resonance Lamps, Technical Note 496, Nat.Bur.Stand.(U.S.A.), US Govt.Print. Off., Washington D.C., USA, 2020.
[21] R. Locht, D. Dehareng, B. Leyh, J. Quant. Spectr. Rad. Transf. 251 (2020) 10748.
[22] M.J. Frisch, G.W. Trucks, H.B. Schlegel, G.E. Scuseria, M.A. Robb, J.R. Cheeseman, G. Scalmani, V. Barone, B. Mennucci, G.A. Petersson, H. Nakatsuji, M. Caricato, X. Li, H.P. Hratchian, A.F. Izmaylov, J. Bloino, G. Zheng, J.L. Sonnenberg, M. Hada, M. Ehara, K. Toyota, R. Fukuda, J. Hasegawa, M. Ishida, T. Nakajima, Y. Honda, O. Kitao, H. Nakai, T. Vreven, J.A. Montgomery Jr., J.E. Peralta, F. Ogliaro, M. Bearpark, J.J. Heyd, E. Brothers, K.N. Kudin, V.N. Staroverov, R. Kobayashi, J. Normand, K. Raghavachari, A. Rendell, J.C. Burant, S.S. Iyengar, J. Tomasi, M. Cossi, N. Rega, J.M. Millam, M. Klene, J.E. Knox, J.B. Cross, V. Bakken, C. Adamo, J. Jaramillo, R. Gomperts, R.E. Stratmann, O. Yazyev, A.J. Austin, R. Cammi, C. Pomelli, J.W. Ochterski, R.L. Martin, K. Morokuma, V.G. Zakrzewski, G.A. Voth, P. Salvador, J.J. Dannenberg, S. Dapprich, A.D. Daniels, O. Farkas, J. B. Foresman, J.V. Ortiz, J. Cioslowski, D.J. Fox, Gaussian 09, Revision A.02, Gaussian Inc., Wallingford CT, 2009.
[23] T.H. Dunning Jr, J. Chem. Phys. 90 (1989) 1007.
[24] J. Cizek, Adv. Chem. Phys. 14 (1969) 35.
[25] G.E. Scuzeria, H.F. Schaefer III, J. Chem. Phys. 90 (1989) 3700.
[26] Y. Zhao, D.G. Truhlar, Theor. Chem. Acc. 120 (2008) 215.
[27] C. Van Caillie, R.D. Amos, Chem. Phys. Lett. 317 (2000) 159.
[28] L. Mei, M. Chuaqui, C.P. Mathers, J.F. Ying, K.T. Leung, Chem. Phys. 188 (1994) 347.
[29] T. Shimanouchi, Tables of Vibrational Frequencies. Consolidated, Vol. 1, NSRDS-NBS 39, 1972.
[30] H.K. Woo, P. Wang, K.C. Lau, X. Xing, C.Y. Ng, J. Chem. Phys. 108 (2004) 9637.
[31] Y.J. Bae, M. Lee, M.S. Kim, J. Phys. Chem. A 110 (2006) 8535.
[32] K. Takeshita, J. Chem.Phys. 110 (1999) 6792.
[33] R. Locht, D. Dehareng, B. Leyh, unpublished results.
[34] (a) P.J. Mohr, B.N. Taylor, D.B. Newell, J. Phys. Chem. Ref. Data 45 (2016) 043102;
(b) P.J. Mohr, D.B. Newell, B.N. Taylor, Rev. Mod. Phys. 88 (2016) 035009.
[35] (a) A.B. Trofimov, I. Powis, R.C. Menzies, D.M.P. Holland, E. Antonsson, M. Patanen, G. Nicolas, C. Miron, A.D. Skitnevskaya, E.V. Gromov, H. Köppel, J. Chem. Phys. 149 (2018) 074306.